Structural Eng. / Earthquake Eng. Vol. 3. No. 1, 83 s-90 s. April 1986
Japan Society of Civil Engineers (Proc. of JSCE No. 368/ I -5)

ANALYSIS OF THIN-WALLED MEMBERS BY FINITE ELEMENT-TRANSFER MATRIX METHOD

By Mitao OHGA and Takashi HARA***

The combined finite element-transfer matrix method is applied to the linear and nonlinear problems of thin-walled members. The transfer matrix is derived from the tangent stiffness matrix used in the FEM. To deal with complex structures the transfer matrix for the substructure, into which thin-walled members is devided, is introduced. In this method, procedures used in the FEM based on load increment are employed except for the estimation of approximate displacements for each specified increment load. Approximate displacement are estimated by the transfer matrix procedure. Some numerical examples presented in this paper show that for long thin-walled members, this method can be successfully applied to the linear and nonlinear problems by reducing the size of the matrix relative to less than that obtained by the FEM.

1. INTRODUCTION

Thin-walled members are analyzed by the finite element method and the finite strip method, etc.. Among these methods, the finite strip method suggested by Cheung[1], which is a formulation of combining the finite element method and Fourier series technique, has the advantage of reducing the size of the matrix in the ordinary finite element method. This method can be successfully applied for the only simple thin-walled members with constant cross sections and particular boundary conditions; otherwise considerable complications arise in the formulation of problems.

The finite element method is the most widely used and powerful tool for analysis of thin-walled members with complex cross-sections[2]. However, the disadvantage of this method is that, in the case of complex and large structures, it is necessary to use a large number of nodes, resulting is very large matrices which require large computers for their management and regulation. In order to overcome this disadvantage of the finite element method, several techniques have been proposed. Sakimoto et al.[3] proposed to reduce the size of the system matrices by using the two types of element, i. e. the plate element and the beam element. The former element was adopted for regions required to be discretized so refined, and the letter for other regions. Okamura et al.[4] analyzed the multi-span plate structures by the stiffness matrix method combined with a relaxation technique. In this approach, the displacement functions in series form and the point-matching method are adopted to derive the stiffness matrix of large-size rectangular plate panels.

Dokainish[5] presented a combined finite element-transfer matrix method for the dynamic analysis of tapered or rectangular plates. In this approach, a finite element formulation was used to obtain the stiffness and mass matrices for a strip of elements whose boundaries were successively connected and

* Member of JSCE, M. Eng., Assoc. Professor of Civil Eng., Ehime University (Matsuyama, Ehime)
** Member of JSCE, Assoc. Professor, Tokuyama College (Tokuyama, Yamaguchi)

whose end boundaries were characterized by state vectors, as defined in the standard transfer matrix method. Since the size of stiffness and mass matrices was equal to the number of degrees of freedom of only one strip, this approach has the advantage of reducing the size of a matrix to less than that obtained by the ordinary finite element method. Ohga et al.[6),7)] followed a similar approach to analyze plate structures with large displacement in elastic and plastic range, and reported that, for long structures in which there are significantly more strips than nodes on section, advantages attainable through matrix size reduction in this method became more evident.

The purpose of this paper is to propose a method of analyzing the elastic-plastic large displacement behavior of thin-walled members under various loading conditions by the combined finite element-transfer matrix method. The substructuring procedure used in the finite element method[8)] is, in this paper, adopted in order to treat complex structures, such as I-section and box-section plate girders with vertical stiffeners and web perforations. In the nonlinear analysis, the same incremental procedures in the finite element method[9)] can be applied, except for the evaluation of incremental load. The Newton-Raphson method is employed in convergence procedures of each iterative step. It is assumed that the Prandtl-Reuss'law, and the von-Mises yield criterion are valid in this paper. In order to consider the extent of the yielded portions in the directions of the cross sections, the cross section of the structure is divided into some layers, and geometric nonlinearity is considered by using a set of moving coordinate systems.

2. FINITE ELEMENT-TRANSFER MATRIX METHOD

As the derivations of the tangent stiffness matrix and the transfer matrix for the plate structure and the descriptions related to the procedure for geometrical and material nonlinear problems are presented in Ref. 6), 7), descriptions which mainly relate to the application of the FETM method to thin-walled members are given here.

(1) Finite element-transfer matrix method for thin-walled members

The thin-walled member is, in the FETM method, divided into some strips, each of which is subdivided into finite elements as shown in Fig. 1. Although two types of strip shown in Fig. 2 may be used, folded strip shown in Fig. 2(a) are used in this paper, since it is expected that, for long structures, advantages attainable through matrix size reduction in folded strips pattern are greater.

Assembling the stiffness matrix of the elements for each strip, the equilibrium equations for the nodes on strip i are obtained as follows:

$$\boldsymbol{F}_i=\boldsymbol{K}_{si}\boldsymbol{\delta}_i \quad (1)$$

in which $\boldsymbol{K}_{si}$=the stiffness matrix of strip i; and $\boldsymbol{\delta}_i$ and $\boldsymbol{F}_i$=the displacement and force vectors of strip i, respectively.

By expanding Eq. (1) and solving for the right displacement vector $\boldsymbol{\delta}^R$ and the force vector $\boldsymbol{F}^R$ in terms of the left displacement vector $\boldsymbol{\delta}^L$ and the force vector $\boldsymbol{F}^L$, the transfer matrix relating the left and right

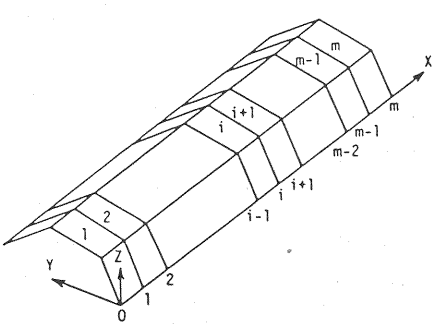

Fig. 1 Subdivision of thin-walled member.

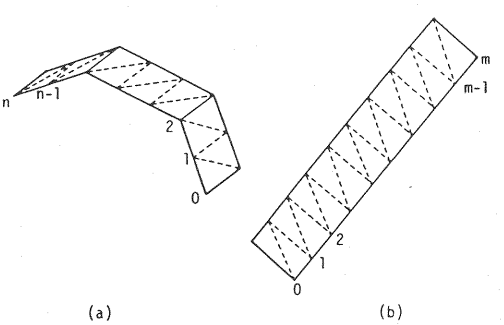

Fig. 2 Strips for thin-walled member.

displacements and forces of the strip can be obtained :

$$\begin{Bmatrix} \delta^R \\ F^R \\ 1 \end{Bmatrix}_i = \begin{bmatrix} -K_{lr}^{-1}K_{ll} & K_{lr}^{-1} & 0 \\ K_{rl}-K_{rr}K_{lr}^{-1}K_{ll} & K_{rr}K_{lr}^{-1} & \overline{F} \\ 0 & 0 & 1 \end{bmatrix}_i \begin{Bmatrix} \delta^L \\ F^L \\ 1 \end{Bmatrix}_i \quad \cdots\cdots (2)$$

or

$$Z_i = T_i Z_{i-1} \quad \cdots\cdots (3)$$

in which K_{ll}, K_{lr}, K_{rl}, and K_{rr}=the sub-matrices of K_{si} ; $\overline{F}$=the load vector acted on the boundary of the strip ; and subscripts L, R indicate the left and right sides of the strip.

(2) Transfer matrix for substructures

In the case of I -section plate girder with vertical stiffeners shown in Fig. 3, there are more nodes on the section with vertical stiffeners than those on the section without vertical stiffener.

The transfer matrix given in Eq. (2) can't be, therefore, employed directly. To overcome this difficulty, I -section plate girder with stiffeners is divided into substructures in which the vertical stiffeners are included as shown Fig. 4 (b), and for each substructure the transfer matrix is derived.

By suitably transforming the stiffness matrix of the substructure, which is obtained by assembling the stiffness matrix of the elements for each substructure, the following equations can be obtained :

$$\begin{Bmatrix} F^L \\ F^I \\ F^R \end{Bmatrix} = \begin{bmatrix} K_{ll} & K_{li} & K_{lr} \\ K_{il} & K_{ii} & K_{ir} \\ K_{rl} & K_{ri} & K_{rr} \end{bmatrix} \begin{Bmatrix} \delta^L \\ \delta^I \\ \delta^R \end{Bmatrix} \quad \cdots\cdots (4)$$

in which, δ^I, and F^I=the displacement and force vectors at inner nodes, respectively ; and K_{ll}, K_{li}, K_{lr}, K_{il}, K_{ii}, K_{ir}, K_{rl}, K_{ri}, and K_{rr}=the sub-matrices of the stiffness matrix of the substructure.

Solving for the δ^I and substituting in the remaining equations, the following expressions are obtained :

$$\begin{Bmatrix} F^L \\ F^R \end{Bmatrix} = \begin{bmatrix} K_{ll}-K_{li}K_{ii}^{-1}K_{il} & K_{lr}-K_{li}K_{ii}^{-1}K_{ir} \\ K_{rl}-K_{ri}K_{ii}^{-1}K_{il} & K_{rl}-K_{ri}K_{ii}^{-1}K_{ir} \end{bmatrix} \begin{Bmatrix} \delta^L \\ \delta^R \end{Bmatrix} + \begin{Bmatrix} K_{li}K_{ii}^{-1}F_i \\ K_{ri}K_{ii}^{-1}F_i \end{Bmatrix} \quad \cdots\cdots (5)$$

or simplifying the notation :

$$\begin{Bmatrix} F^L \\ F^R \end{Bmatrix} = \begin{bmatrix} K_{11} & K_{12} \\ K_{21} & K_{22} \end{bmatrix} \begin{Bmatrix} \delta^L \\ \delta^R \end{Bmatrix} + \begin{Bmatrix} F_1 \\ F_2 \end{Bmatrix} \quad \cdots\cdots (6)$$

By expanding and rearranging Eq. (6), it can be shown after various matrix manipulations that the left and right boundaries can be related by the following expression :

$$\begin{Bmatrix} \delta^R \\ F^R \end{Bmatrix} = \begin{bmatrix} -K_{12}^{-1}K_{11} & K_{12}^{-1} \\ K_{21}-K_{22}K_{12}^{-1}K_{11} & K_{22}K_{12}^{-1} \end{bmatrix} \begin{Bmatrix} \delta^L \\ F^L \end{Bmatrix} + \begin{Bmatrix} -K_{12}^{-1}F_2 \\ F_2-K_{22}K_{12}^{-1}F_1 \end{Bmatrix} \quad \cdots\cdots (7)$$

or simplifying the notation :

$$\begin{Bmatrix} \delta^R \\ F^R \end{Bmatrix} = \begin{bmatrix} T_{11} & T_{12} \\ T_{21} & T_{22} \end{bmatrix} \begin{Bmatrix} \delta^L \\ F^L \end{Bmatrix} + \begin{Bmatrix} T_{F_1} \\ T_{F_2} \end{Bmatrix} \quad \cdots\cdots (8)$$

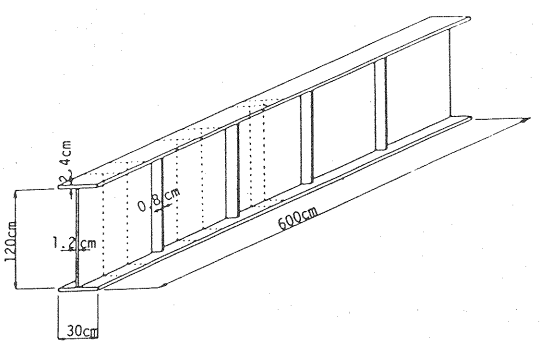

Fig. 3 I -section plate girder with vertical stiffeners.

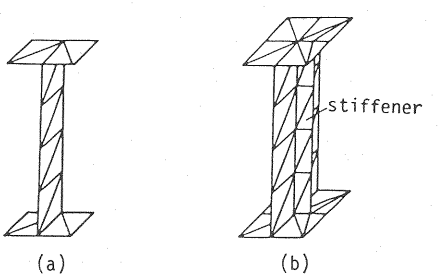

Fig. 4 Strips for I -section plate girder with vertical stiffeners.

Adding one dummy equation to the system, the following equation can be obtained :

$$\begin{Bmatrix} \delta^R \\ F^R \\ 1 \end{Bmatrix} = \begin{bmatrix} T_{11} & T_{12} & T_{F_1} \\ T_{21} & T_{22} & T_{F_2} \\ 0 & 0 & 1 \end{bmatrix} \begin{Bmatrix} \delta^L \\ F^L \\ 1 \end{Bmatrix} \quad \cdots\cdots (9)$$

which is the expanded transfer matrix relating the state vectors of the left and right boundaries of a substructure through the intermediate degrees of freedom. The sizes of the state vector and transfer matrix in Eq. (9) are same as those of the state vector and transfer matrix for the strip without the vertical stiffener shown in Fig. 4 (a). Both transfer matrices can be, therefore, maltiplied each other. I -section plate girder shown in Fig. 3 can be analyzed by the combined use of the transfer matrix for the strip without vertical stiffener and that for the substructure with stiffeners.

(3) Transformation for nodal displacements

In the determining an equilibrium configuration of the structure under a given set of loads, the current local displacements which are related to the displaced local coordinate axes x, y, z, shown in Fig. 5, are used to determine the local nodal forces. The local displacements are established by the transformation of nodal displacements from the global coordinate system to the local coordinate system. The transformation procedure for displacements $U=\{u, v, w\}$ employed in this paper is same as that for plate structures, and is described in Ref. 9). Hence, only descriptions of the transformations of rotations are presented here.

A typical element before and after deformation is shown in Fig. 5. Four sets of rectangular cartesian axes : (1) The global coordinate system (X, Y, Z);(2) the initial local coordinate system (x^*, y^*, z^*);(3) the displaced local coordinate system (x, y, z);(4) the coordinate system (X^*, Y^*, Z^*), which is established by the parallel transformation of the initial local coordinate system, such that the origin of this coordinate system is coincide with that of the global coordinate system are defined. Assuming that $\boldsymbol{E}$, $\boldsymbol{e}^*$, $\boldsymbol{e}$, and $\boldsymbol{E}^*$ indicate the unit orthogonal vectors in above coordinate systems, respectively, the following expressions are obtained :

$$\boldsymbol{e}=\boldsymbol{L}_A\boldsymbol{E}, \quad \boldsymbol{e}^*=\boldsymbol{L}_B\boldsymbol{E}, \quad \boldsymbol{E}^*=\boldsymbol{L}_B\boldsymbol{E} \quad \cdots\cdots (10)$$

in which $\boldsymbol{L}_A$, and $\boldsymbol{L}_B$=the rotation matrices between the global coordinate system and the displaced coordinate system, and the global system and the initial system, respectively.

S′ designates a point S after deformation and S″ indicates a point S in the reference element established on the displaced local axes having the same shape and size as the original element. As shown in Fig. 5, the vector $\rho=\overrightarrow{0S'}$ may be described in two ways :

$$\rho=\overrightarrow{01}+\overrightarrow{1S}+\overrightarrow{SS'} \quad \cdots\cdots (11)$$

or

$$\rho=\overrightarrow{01}+\overrightarrow{1'1}+\overrightarrow{1'S''}+\overrightarrow{S''S'} \quad \cdots\cdots (12)$$

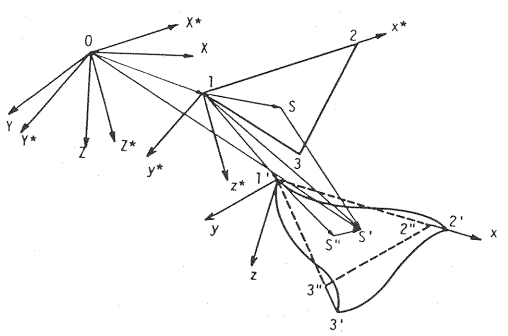

Fig. 5 Location of element before and after deformation.

Expressing as componets related to the coordinate system (X^*, Y^*, Z^*), Eqs. (11) and (12) become :

$$\begin{Bmatrix} X^* \\ Y^* \\ Z^* \end{Bmatrix} = \begin{Bmatrix} X_1^* \\ Y_1^* \\ Z_1^* \end{Bmatrix} + \begin{Bmatrix} x_0 \\ y_0 \\ 0 \end{Bmatrix} + \begin{Bmatrix} U^* \\ V^* \\ W^* \end{Bmatrix} \quad \cdots\cdots (13)$$

$$\begin{Bmatrix} X^* \\ Y^* \\ Z^* \end{Bmatrix} = \begin{Bmatrix} X_1^* \\ Y_1^* \\ Z_1^* \end{Bmatrix} + \begin{Bmatrix} U_1^* \\ V_1^* \\ W_1^* \end{Bmatrix} + \boldsymbol{L}^T \begin{Bmatrix} x_0 \\ y_0 \\ 0 \end{Bmatrix} + \boldsymbol{L}^T \begin{Bmatrix} u \\ v \\ w \end{Bmatrix} \quad \cdots\cdots (14)$$

in which $\boldsymbol{L}$=the rotation matrix between the initial coordinate system and the displaced coordinate system, i. e. $\boldsymbol{L}=\boldsymbol{L}_A\boldsymbol{L}_B^T$

Solving the last line of Eq. (14) for w, and recognizing from Eq. (13) that $W^*=Z^*-Z_1^*$, the following expression can be obtained :

$$w=L_{31}(X^*-X_1^*-U_1^*)+L_{32}(Y^*-Y_1^*-V_1^*)+L_{33}(W^*-W_1^*) \quad \cdots\cdots (15)$$

in which L_{31}, L_{32}, and L_{33}=the components of the rotation matrix $\boldsymbol{L}$, respectively.

By differentiating both sides of Eq. (15) by x and y, respectively, the following expressions can be obtained :

$$\left.\begin{aligned}\frac{\partial w}{\partial x}&=\frac{\partial w}{\partial X^*}\cdot\frac{\partial X^*}{\partial x}+\frac{\partial w}{\partial Y^*}\cdot\frac{\partial Y^*}{\partial x}\\ \frac{\partial w}{\partial y}&=\frac{\partial w}{\partial X^*}\cdot\frac{\partial X^*}{\partial y}+\frac{\partial w}{\partial Y^*}\cdot\frac{\partial Y^*}{\partial y}\end{aligned}\right\} \quad \cdots\cdots (16)$$

in which

$$\frac{\partial w}{\partial X^*}=L_{31}+L_{33}\frac{\partial W^*}{\partial X^*},\quad \frac{\partial w}{\partial Y^*}=L_{32}+L_{33}\frac{\partial W^*}{\partial Y^*}$$

Considering that, in the displaced coordinate system $(x,\ y,\ z)$, $x=x_0+u$ and $y=y_0+v$, the following expressions are obtained from Eq. (14) :

$$\left.\begin{aligned}X^*&=X_1^*+U_1^*+L_{11}x+L_{21}y+L_{31}w\\ Y^*&=Y_1^*+V_1^*+L_{12}x+L_{22}y+L_{32}w\end{aligned}\right\} \quad \cdots\cdots (17)$$

Differentiating both sides of Eq. (17) by x and y, respectively, and substituting $\partial X^*/\partial x$, $\partial X^*/\partial y$, $\partial Y^*/\partial x$, and $\partial Y^*/\partial y$ obtained above into Eq. (16), the rotational transformations are finally established as follows :

$$\left.\begin{aligned}\theta_x&=\{(L_{31}-L_{33}\theta_Y^*)L_{21}+(L_{32}+L_{33}\theta_X^*)L_{22}\}/\alpha\\ \theta_y&=-\{(L_{31}-L_{33}\theta_Y^*)L_{11}+(L_{32}+L_{33}\theta_X^*)L_{12}\}/\alpha\end{aligned}\right\} \quad \cdots\cdots (18)$$

in which

$$\theta_X^*=\partial W^*/\partial Y^*,\quad \theta_Y^*=-\partial W^*/\partial X^*$$

$$\alpha=1-(L_{31}-L_{33}\theta_Y^*)L_{31}-(L_{32}+L_{33}\theta_X^*)L_{32}$$

It is confirmed by the authors that the solutions obtained by the procedure described here are, in the plate structure problems, exactly coincide with those obtained by Komatsu's procedure[9].

3. NUMERICAL EXAMPLES

a) Box-section plate girder

To examine the accuracy and efficiency of the FETM method, a box-section plate girder loaded at the midspan shown in Fig. 6 is analyzed, and the results obtained by the FETM method are compared with those obtained by the finite element method, where the same element and mesh pattern as those used in the FETM method are employed.

In the numerical calculation, a quarter of the entire system is divided into 4, 6, 8, and 10 strips, and each strip into 8 triangular elements for every dividing patterns. Neither geometrical nor material nonlinearity is, herein, taken into consideration, and both edge boundaries are assumed to be fixed.

Fig. 7 (a) shows a comparison between the deflections at the point C in Fig. 6 obtained by the FETM method and those obtained by the finite element mthod. As shown Fig. 7 (a), both results coincide within three significant figures with each other. Fig. 7 (b) shows a comparison of computation times of both methods in this example. It can be seen that, in computation time, although the FETM method has less advantage for the small number of strips pattern (4 and 6 strips pattern), this method has much advantage for the large number of strips pattern (8 and 10 strips pattern). Fig. 7 (c) shows a comparison of the matrix sizes required in both methods. The matrix size in the finite element method increses as the number of strips, i. e. the number of total nodes increases, and if the banded matrix is used, it is given by {(the number of total nodes) × (degress of freedom)}× (the band width). The matrix to be considered in the finite element method for this example is, therefore, 25×6×42=6 300 for 4-strips pattern, 35×6×42=8 820 for 6-strips pattern, 45×6×42=11 340 for 8-strips pattern, and 55×6×42=13 860 for 10-strips pattern in this example. On the other side, the matrix size in the FETM method is dependent on the number of degrees of freedom for only one strip in contrast with the finite element method, and it is given by {(the

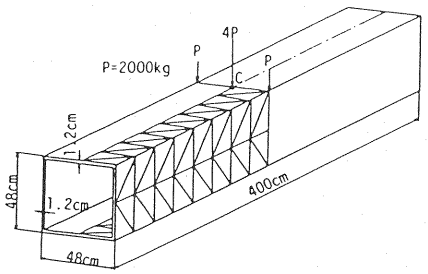

Fig. 6 Box-section plate girder.

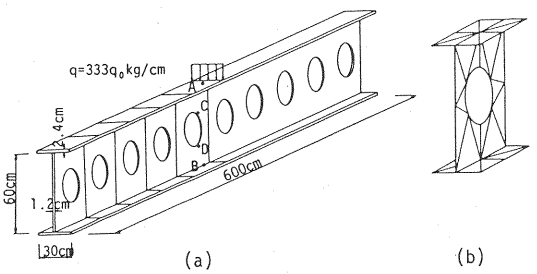

Fig. 8 I-beam with web perforations.

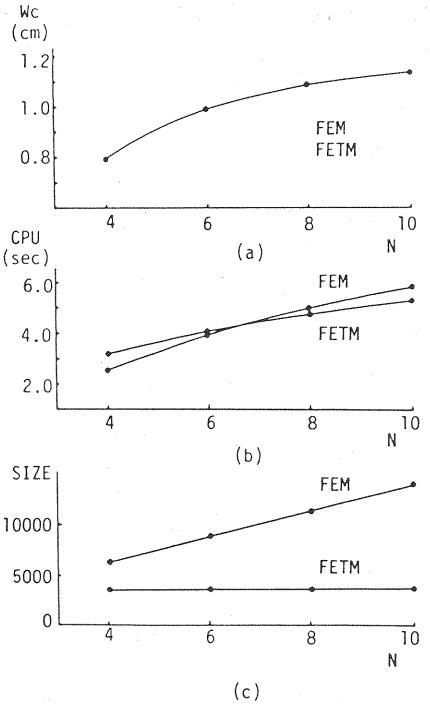

Fig. 7 Comparison of FETM and FEM.

number of nodes on a section) × (degrees of freedom) $\times 2]^2$. The matrix to be considered in the FETM method is, $(5\times6\times2)^2=3\,600$ for every dividing patterns.

b) I-section beam with web perforations

To illustrate the efficiency of the FETM methods based on the substructuring procedure developed in this paper, I-section beam loaded at the midspan with consecutive web perforations, as shown in Fig. 8 (a), is analyzed, and numerical results are compared with those obtained by the finite element method. The half member is divided into five same substructures, and each substructure into 30 triangular elements, as shown in Fig. 8 (b). Among all the 26 nodes of each substructure, 12 nodes are inner nodes. Geometrical and material nonlinearity are taken into consideration, and the modulus of elasticity $E=2.1\times10^6$ kg/cm^2, the yield stress $\sigma_Y=2\,800$kg/cm^2, and the poisson's ratio $\nu=0.3$ are used for calculation. Other dimensions are indicated in Fig. 8 (a), and both edge boundaries are assumed to be fixed, as in the previous example.

Fig. 9 shows the center deflections of the upper and lower flanges at $x=0.1\,L$, $0.3\,L$, and $0.5\,L$. In Fig. 9, the finite element solutions are also shown, and both results coincide with each other. The deflections at $x=0.1\,L$ and $0.3\,L$ increase almost linearly, and very little difference exists between the deflections of the upper and lower flanges, so that it is can't be distinct in Fig. 9. On the other hand, the deflection of the upper flange at $x=0.5\,L$ increases nonlinearly from load level $q=2.5$ and is greater compared with that of the lower flange.

Fig. 10 shows the out-of-plane displacements of midpoint of web at $x=0.1\,L$, $0.2\,L$, $0.3\,L$, $0.4\,L$, and $0.5\,L$. Good agreement exists between the results obtained by the FETM method and the finite element method as the deflections of the flange.

Fig. 11 and 12 show the axial stresses of the upper and lower flange (A and B in Fig. 8), and the axial stresses of the web (C and D in Fig. 8). Both the results of the FETM method and the finite element method are also in good agreement.

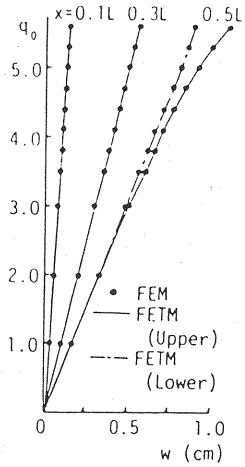

Fig. 9 Deflections at upper and lower flange.

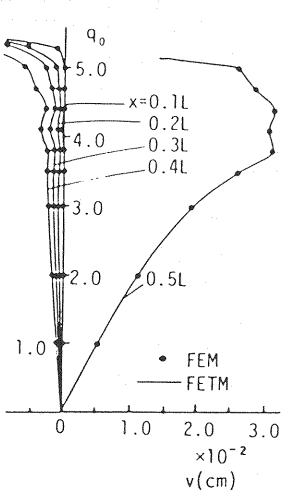

Fig. 10 Out-of-plane displacements at midpoint of web.

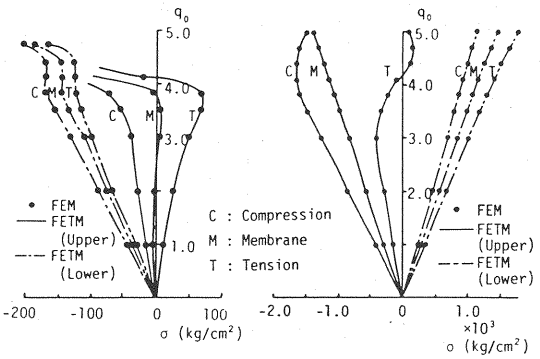

Fig. 11 Stresses at upper and lower flange.

Fig. 12 Stresses at web.

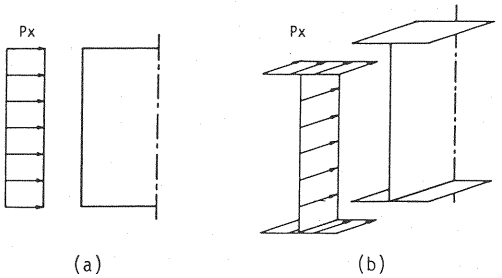

Fig. 13 Models for analysis.

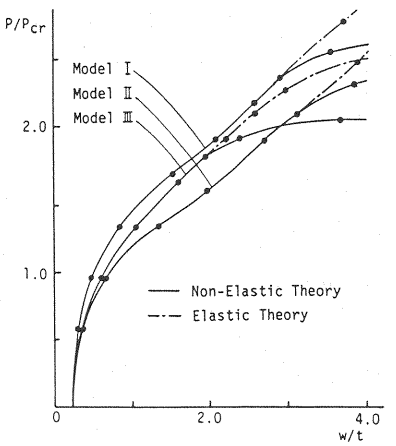

Fig. 14 Deflections at midpoint of center web.

The matrix to be considered in the finite element method is, if the banded matrix is used, 726×84 for this example, compared to 84×84 in the FETM method.

c) I-section plate girder with stiffeners under inplane axial load

For the last example, stiffened I-section plate girder subjected at the edges to inplane axial load, as shown in Fig. 3, is analyzed. Numerical calculations are, in this example, proceeding for the following three models. (1) Model I; a model composed of only a sub-panel between the vertical stiffeners, shown in Fig. 13(a). It is assumed that, in this model, both side boundaries are simply supported, and upper and lower boundaries are fixed. (2) Model II; a model cut out from entire structure by two adjacent vertical stiffeners shown in Fig. 13(b). In this model, the effects of the flanges on the behaviors of the structure can be, therefore, taken into consideration, and side boundaries are assumed to be fixed as in Model I. (3) Model III; a total system model of the I-section plate girder, shown in Fig. 3. In this model, not only the effects of the flanges but also of the stiffeners can be taken into consideration, and both edge boundaries are assumed to be fixed.

In Models I and II, the initial deflection of plate bending mode is assumed, and defined as follows:

$$w_0=\overline{w}_0 \sin\frac{\pi}{a}x \sin\frac{\pi}{b}y \quad \cdots\cdots (19)$$

in which $\overline{w}_0$=the maximum value of initial deflection and here $\overline{w}_0=t/5$ is assumed. On the other hand, in Model III the initial deflection given above is assumed for every sub-panels between the vertical stiffeners. The yield stresses of the web and flanges are assumed to be σ_Y=2 800 kg/cm² and the yield stress of the

vertical stiffener σ_{sY} is 4 000 kg/cm^2, and other material constants are same as those in the previous example. The half member is, in Model Ⅲ, divided into 6 substructures, and each substructure into triangular finite elements as shown in Fig. 4(a), (b).

Fig. 14 shows the out-of-plane displacements at the midpoint of web, where the displacement for Model Ⅲ is of the center web. It is shown from Fig. 14 that until the load level of about 2.0 the load-deflection curves for every models show similar tendencies, and the deflection for Model Ⅱ is greatest, and that for Model Ⅲ is next. Since over this load level, in Models Ⅰ and Ⅱ, the effects of the geometrical nonlinearity on the behaviors of the Ⅰ-section plate girder become substantial, the increasing rate of the deflections for Models Ⅰ and Ⅱ become smaller. On the other hand, the deflection for Model Ⅲ increases suddenly in contrast with Models Ⅰ and Ⅱ, and the ultimate strength for Model Ⅲ is approximately 20 % less than that for Model Ⅰ.

4. CONCLUSIONS

The combined finite element-transfer matrix method is applied to the linear and nonlinear problems of thin-walled members, and a computer program based on this theory has been developed. The following conclusions can be drawn from this study:

(1) Good agreement exists between the results obtained by the FETM method and the finite element method not only in the linear problems but also in the nonlinear problems, which demonstrates the accuracy of the proposed method.

(2) From numerical examples presented in this paper, it is shown that this method can be successfully applied to the long thin-walled members by reducing the size of the matrix and the computation time relative to less than that obtained by the finite element method.

(3) By adopting the transfer matrix for substructures derived in this paper, complex thin-walled members, such as Ⅰ-section and box-section plate girders with vertical stiffeners and web perforations, can be treated easily.

(4) Considerable differences exist between the results for the model of entire system and for the model cut out from the structure.

REFERENCES

1) Cheung, Y. K.: Finite Strip Method in Structural Analysis, Pergamon Press, 1976.
2) Zienkiewicz. O. C.: The Finite Element Method in Engineering Science, McGraw-Hill, 1971.
3) Yamamoto, T., Hotta, M., Obata, K. and Sakimoto, T.: Analysis of Thin-Walled Structures by Combined Use of Plate and Beam Elements, 38th Annual Conference of JSCE, pp. 155~156, Oct., 1983 (in Japanese).
4) Okamura, H. and Ishikawa, K.: Analysis of Multi-Span Plate Structures by a Small Computer, Proc. of JSCE, No. 344/Ⅰ-1, pp. 313~322, April, 1984 (in Japanese).
5) Dokainish, M. A.: A New Approach for Plate Vibrations: Combination of Transfer Matrix and Finite-Element Technique, Transactions, Journal of Engineering for Industry ASME, Vol. 94, No. 2, pp. 526~530, 1972.
6) Ohga, M., Shigematsu, T. and Hara, T.: Structural Analysis by a Combined Finite Element-Transfer Matrix Method, An International Journal of Computers and Structures, Pergamon Press, London, England, Vol. 17, No. 3, pp. 321~326, 1983.
7) Ohga, M., Shigematsu, T. and Hara, T.: A Combined Finite Element-Transfer Matrix Method, Journal of the Engineering Mechanics Division, ASCE, Vol. 110, No. EM9, pp. 1335~1349, 1984.
8) McGuire, W. and Gallagher, R. H.: Matrix Structural Analysis, John Wiley & Sons, 1979.
9) Komatsu, S., Kitada, T. and Miyazaki, S.: Elastic-Plastic Analysis of Compressed Plate with Residual Stress and Initial Deflection, Proc. of JSCE, No. 244, pp. 1~14, Dec., 1975 (in Japanese).

(Received June 12 1985)